Modelling of dissolved H in Ga stabilised δ-Pu

Chris Scott*, Steven D. Kenny

*Department of Mathematical Sciences, Loughborough University, Leicestershire,
LE11 3TU, UK*

Mark T. Storr, Andrew Willetts

Atomic Weapons Establishment, Aldermaston, Reading, RG7 4PR, UK

Abstract

The behaviour of hydrogen in Ga stabilised δ-Pu has been investigated using atomistic computer simulation techniques. We have considered only the solid solution of H in Pu-Ga. H diffusivity in the undamaged material was calculated and was shown to depend on the Ga concentration of the Pu-Ga alloy. Furthermore, localised regions of high Ga concentration within the material were shown to block H diffusion pathways. These are important findings and could allow for the possibility to control H diffusion if it were possible to control the Ga configuration within the system. The interaction of H with simple point defects was also investigated and suggests that H will behave differently in cascade damaged systems compared to undamaged systems. Vacancies were observed to trap any H interstitials that enter their vicinity, while the likelihood of dissociation was very low, effectively reducing the H diffusion coefficient to zero. On the other hand, binding energy calculations show that it is energetically unfavourable for a H interstitial to be close to a Pu interstitial. No long range interaction between H and the single point defects was observed.

Keywords: Plutonium, MEAM, Radiation damage, Hydrogen diffusion

*Corresponding author
Email address:* `C.D.J.Scott@lboro.ac.uk` (Chris Scott)

1. Introduction

Plutonium is an important nuclear material that has been the subject of scientific research, both experimental and theoretical, for decades [1, 2], and in which there is interest in both the chemical and physical behaviour. For example, where plutonium is stored, potentially for many years, it is important to understand how it might physically change so that it can be safely removed from storage. The underlying causes of change, including radiation damage, can lead to a number of complicated, potentially interconnected effects, such as the creation of defects, helium in-growth and daughter product in-growth, making the prediction of overall change difficult. A particular challenge is to understand how the chemistry of plutonium is determined by its electronic structure; this is made particularly difficult by the strong electron correlation of the 5f electrons. This, combined with other issues such as relativistic effects, makes electronic structure theory methods, such as density functional theory, more complicated to apply in order to achieve reasonable predictive accuracy. In addition, there are a number of issues with performing experiments with plutonium, including both its radioactivity and its availability. Hence, there are many opportunities and benefits in developing and using atomistic computer simulation techniques to investigate and ultimately understand plutonium.

The particular focus of this paper is to understand the behaviour of hydrogen in aged plutonium. In order to do this we need to consider not only how the plutonium might change, but also how hydrogen interacts with it. This will be examined through calculation of the hydrogen diffusivity, which is reasonably straightforward to calculate and delivers the initial understanding we require. For example, we expect the way in which hydrogen interacts with different defects in the system, such as vacancies and interstitials caused by radioactive decay, to influence its diffusivity. In this paper we will consider only point defects, although the understanding gained may be useful in future interpretation of hydrogen interaction with bulk defects, for example grain boundaries.

Hydrogen diffusion is a technologically important property in many metals due to the possibility of effects such as hydrogen embrittlement [3] and stress corrosion cracking [4]. Experimental diffusion coefficients for metals with a face-centred cubic structure typically show values spread over many orders of magnitude, as in Al [5], although some show more reasonable consistency across experimental groups, for example Ni [6]. Atomically, hydrogen

diffusion occurs by a series of jumps between interstitial sites in the face-centred cubic structure. Both octahedral and tetrahedral interstitials will be considered here. Trapping of hydrogen in the neighbourhood of different defects (dislocations, vacancies and voids) has been used to explain the large discrepancies in the experimental Al data.

Considering the simulation system in more detail, of interest in this study is the δ phase of plutonium, which has a face-centred cubic structure. Although pure plutonium is not stable in this phase at room temperature, the addition of certain elements such as Al, Am, Ce and Ga, has been shown to have a stabilising effect. It is the Pu-Ga combination which will be modelled here; there are many benefits to looking at Pu-Ga including experimental data for comparison [7], continuity with studies previously performed [8] and access to an appropriate MEAM potential [9]. Additionally, such a study may give some insight into the optimum practical inclusion of further elements, such as uranium arising from the radioactive decay process, as this becomes necessary to further refine our understanding.

There have been a number of previous studies involving the atomistic modelling of plutonium [10]. Many have used the Modified Embedded Atom Method (MEAM) [11], which has been extended from pure plutonium to include Ga [12] and He [13], to model the interatomic interactions. A further extension was therefore introduced here to include hydrogen. In order to represent the aged plutonium structure we will only consider the results of a radiation decay event. Plutonium undergoes alpha decay leading to the creation of a uranium atom. Both the heavy uranium atom and the alpha particle cause defects in the metal lattice, with the majority being caused by the uranium recoil. The alpha particle is subsequently trapped as a helium atom. Previous work has comprehensively investigated the ballistic phase of radiation events in δ-Pu [14, 15] and the formation and mobility of point defects [16, 17, 18]. The formation and diffusion of He in a Pu-Ga system has also been considered, along with the formation of He bubbles [8, 13].

Other authors have also previously studied H in Pu systems. Schwartz et al have investigated hydrogen-vacancy effects in Pu-Ga alloys using experimental and *ab initio* calculations [19]. They have shown a strong binding between a H and a vacancy and that the formation energy of the complex drops further as more H atoms are added to the vacancy (up to 4 H in one vacancy were considered). Density functional theory (DFT) calculations have been performed on H in δ-Pu by Taylor et al [20]. The authors have investigated H behaviour at surfaces, interstitial and vacancy locations and

3

at a grain boundary, and have also shown that a H will bind to a vacancy. Wei et al have modelled H diffusion in pure δ-Pu using DFT [21]. They have shown that the octahedral interstitial location has a slightly lower energy than the tetrahedral location and that the H is likely to diffuse between neighbouring interstitial locations. The lowest energy transition they found was tetrahedral to octahedral, followed by octahedral to tetrahedral and then tetrahedral to tetrahedral.

Here the diffusivity of a hydrogen atom through both a reference undamaged Pu-Ga system and one including a single point defect (both a plutonium interstitial and vacancy are considered) will be calculated. Hence this study will address two specific aspects of hydrogen interaction with the aged system, namely the effect of point defects and that of gallium. The influence of helium on hydrogen diffusivity is not specifically included in this study, as we feel that it is important to gain a good understanding of the behaviour of hydrogen in the presence of point defects before introducing further complication to the system. A similar argument holds for the introduction of uranium into the simulation system.

2. Methodology

Throughout this work Pu-Ga self and cross interactions were modelled using the MEAM potential. This potential has the form:

$$E_i = F_i(\rho) + \frac{1}{2} \sum_i \phi(R_{ij}), \tag{1}$$

where E_i is the energy of atom i, $F_i(\rho)$ is the embedding energy of atom i, determined from the surrounding environment, and ϕ is a pair potential chosen so as to give the correct equation of state. Parameters were taken from reference [13]. Previous work has shown this potential to accurately capture the complexities of the Pu phase diagram [12, 16, 17, 22, 23]. H-H self interactions were also modelled by the MEAM potential, which was developed to model H in metals [24] and allows for the formation of a H_2 molecule. At close particle separations the pair potential component of the MEAM potential, ϕ, was replaced by the ZBL screened Coulomb potential [25]. This potential represents the repulsion of the nuclei and is known to be very accurate at close particle separations. An exponential spline function was used to spline the pair potentials together. Valone and Baskes published

4

a correction to the Pu-Pu MEAM potential [26] in which both the pair and embedding terms were switched to a ZBL potential at close range (as opposed to just the pair term). This change is especially important when considering high energy cascades. However, since we are only performing diffusion simulations the kinetic energies of atoms will not be high enough that the ZBL component will be used (atoms will not get that close to one another), so we have not applied this correction.

This leaves only the Pu-H and Ga-H interactions. Due to the lack of experimental and ab initio data on these interactions we approximated them with the purely repulsive ZBL potential with a cut-off of 3.5 Å. Thus there was no attractive element to these potentials. As a result of this there is no possibility of the formation of the hydride and this limits the validity of our results to the solid solution portion of the phase diagram. Therefore in this work we will only consider very low concentrations of H. In the future we aim to extend our model to allow for bonding between Pu/Ga-H.

When constructing Pu-Ga systems we must consider the Ga ordering within the system. Throughout this work we created the systems by first creating a Pu_3Ga lattice ($L1_2$ space group) and then randomly replacing Ga atoms with Pu atoms until the desired Ga concentration was reached. This guaranteed at least second nearest neighbour spacing; Ga-Ga first nearest neighbour bonds are unfavourable [27]. Unless otherwise mentioned we always created Pu 5 at. % Ga systems since this is the concentration we have considered previously [14, 16] and it falls centrally within the stable concentration bounds of 2 and 9 % at ambient temperature [28]. Periodic boundary conditions were employed throughout.

Average energy differences between various H-Pu/Ga interstitial configurations were calculated using the following equation:

$$E_f = E_T^{def} - N_{Pu}^{def} E_{Pu}^{bulk} - N_{Ga}^{def} E_{Ga}^{bulk}, \tag{2}$$

where E_f is the average energy of the given configuration, E_T^{def} is the total energy of the defective system, N_{xx}^{def} is the number of atoms of specie xx = Pu or Ga in the defective system and E_{xx}^{bulk} is the bulk energy per atom for specie xx = Pu or Ga. To ensure good statistics a large number of 864 atom Pu-Ga configurations were considered. For each type of defect we took 50 different Pu-Ga configurations and within each configuration we took 50 different sites for the defect, a total of 2,500 unique sites. Once the defect was constructed the energy of the system was minimised using the L-BFGS method [29] to

give E_T^{def}. The bulk energy per atom values were calculated as an average over the 50 Pu-Ga configurations.

Transition energy barriers were calculated using the climbing image Nudged Elastic Band (NEB) method [30] using 15 images (13 moving). As with the energy difference calculations, we took 50 Pu-Ga configurations, each containing 864 atoms, with 50 sites in each, which resulted in a total of $2,500$ calculations per transition. The initial and final points of the transition were manually constructed so as to study specific pathways, for example the octahedral to octahedral interstitial pathway.

The diffusivity of H in undamaged Pu-Ga was calculated from the time dependence of the mean square displacement (MSD), using the following Einstein relation:

$$D(T) = \frac{\langle R^2(t) \rangle_T}{2dt}, \tag{3}$$

where D is the diffusion coefficient, $\langle R^2(t) \rangle_T$ is the mean square displacement at temperature T, $d = 3$ is the dimension and t is time.

In order to obtain good statistics during the MSD calculation we used between 24 and 56 different Pu-Ga configurations, depending on the temperature of the simulation. For lower temperatures we did more simulations since the diffusivity was lower and hence more difficult to calculate accurately. The Pu-Ga systems contained $16,384$ atoms to which we added 8 well separated H interstitials. This low concentration of H minimises the probability of H atoms interacting with one another during the simulations. Initially the systems were thermalised to the desired temperature using the Berendsen thermostat [31], over a time of 12 ps. At this point the thermostat was turned off and a NVE ensemble molecular dynamics (MD) simulation was performed for 3 ps, to ensure we have a correct distribution of velocities initially. After this point the MSD calculation began. The simulations were performed until a time of 100 ps was reached and the value of the MSD was evaluated and stored at intervals of 0.125 ps.

The diffusion coefficient, D, was obtained from the gradient of the MSD curves, using Equation 3. Assuming Arrhenius behaviour, the effective migration energy barrier could then be calculated from the Arrhenius equation:

$$D(T) = \nu \exp\left(-\frac{E_m}{k_B T}\right), \tag{4}$$

where ν is the prefactor, E_m is the effective migration energy barrier and k_B

the Boltzmann constant. E_m was calculated from the gradient of the linear fit to the Arrhenius plot of $\ln D$ against $1/T$.

The diffusivity of H in systems containing a single Pu point defect was also considered. These simulations were similar to the H diffusivity simulations in undamaged Pu-Ga with the addition of a single point defect. We considered simulations at a temperature of 700 K only, with the systems thermalised in the same way as for the undamaged material. We carried out 448 simulations in total, arising from 112 Pu-Ga configurations containing $2,048$ atoms with 4 different H-defect separations in each; namely 0-4, 4-8, 8-12 and 12-16 Å. This gave a good distribution of initial separations. The simulations were run for a time of 300 ps.

To calculate the binding energy of two defects we calculated the formation energy of the adjacent defects and compared this to the formation energy of the well separated, individual defects. A negative binding energy indicated the adjacent configuration was more favourable and vice versa. To calculate the formation energy of two well separated defects we simply added the formation energies of the individual defects. To calculate the energy of adjacent defects we took 250 different $2,048$ atom Pu-Ga configurations and in each configuration we took 100 different Pu vacancy sites. For each site we took 3 different H positions with separations 0-4, 4-8 and 8-12 Å. This resulted in $75,000$ calculations in total and ensured a good distribution of separations. The energy of the adjacent defects was calculated using Equation 2. The difference of this energy and the energy of the separated defects is the binding energy.

3. Results

In the following sub-sections we have displayed the results of our calculations regarding H in δ-Pu. Initially we have performed statics calculations on various H configurations within the system and have also calculated transition barriers for H interstitial diffusion. We have then proceeded to investigate H diffusivity in the undamaged material, initially with a Ga concentration of 5 at. %, and subsequently over a range of Ga concentrations. Finally we have investigated the behaviour of H near simple point defects, namely a vacancy and a Pu split interstitial, and their effect on the diffusivity of H.

Defect structure	Energy (eV)
H subs (-1 Pu)	0.0 (0.69)
H octa	1.18 ± 0.09 (1.87)
H tetra	1.20 ± 0.18 (1.89)
Pu (100) + H subs	1.4 ± 0.05 (2.09)
Pu octa + H subs	1.49 ± 0.68 (2.18)
Pu tetra+ H subs	1.62 ± 0.79 (2.31)

Table 1: The average energy difference between various H-Pu/Ga interstitial configurations, taking the H substitutional case as a reference. Values in brackets use the perfect lattice as a reference. Calculations were carried out in Pu 5 at. % Ga and were averaged over $2,500$ unique sites. Subs stands for substitutional and octa and tetra for the octahedral and tetrahedral interstitial locations respectively. Pu (100) refers to a Pu (100)-oriented split interstitial.

3.1. Statics calculations

We have initially performed calculations on the energetics of H in the Pu-Ga lattice to gain an understanding of how H may diffuse through the material. Table 1 shows the average energy difference between a number of H-Pu/Ga interstitial configurations in Pu 5 at. % Ga. It is clear that when H was in an interstitial location (1.18, 1.2 eV) the energy was lower than the cases when H was substitutional with a neighbouring Pu interstitial (1.4, 1.49, 1.62 eV). This implies that H will remain in an interstitial location rather than force Pu off lattice and sit substitutionally, and also suggests that H diffusion between interstitial locations is possible. Interestingly, this differs from the behaviour of He in Pu, where the energy of the substitutional defect is lower and a He atom in an interstitial location will push a Pu atom off-lattice and sit in the substitutional site [8].

In order to determine the likelihood of H interstitial diffusion, transition barriers were calculated for H interstitials moving between neighbouring interstitial locations, with the resulting distributions shown in Figure 1. From the distributions it is clear there was a large variance in the barriers, due to the presence of Ga. For example, a transition involving a H interstitial moving from a site neighboured by a Ga atom to a site further from the Ga atom, would have a much lower barrier than a H moving in the opposite direction, due to the disruption the H causes to the energetically favourable Pu-Ga bonds. The lower energy transitions from the distributions occur much more frequently than higher energy ones, suggesting that octahedral to tetrahe-

(a) Octahedral to octahedral

(b) Octahedral to tetrahedral

(c) Tetrahedral to tetrahedral
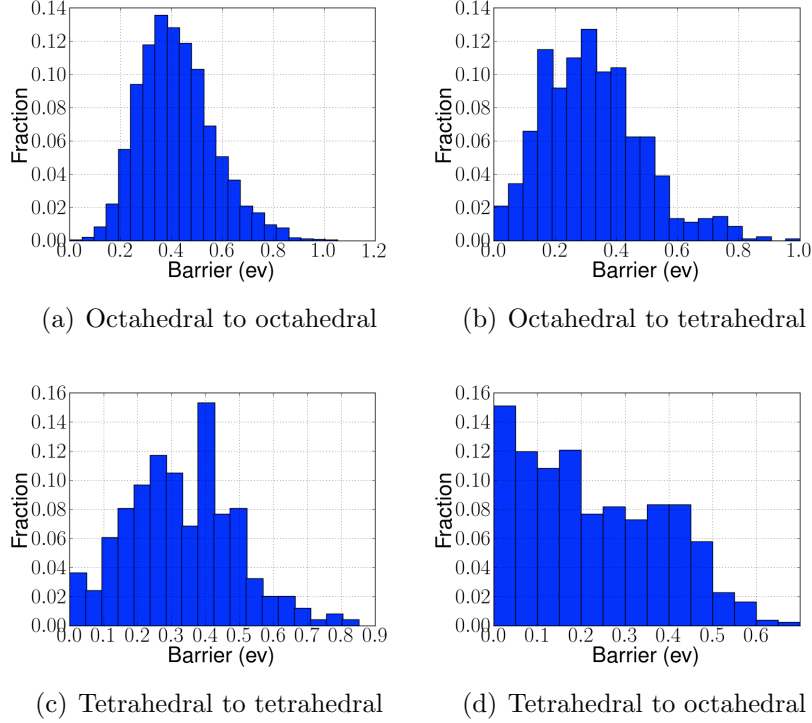
(d) Tetrahedral to octahedral

Figure 1: Distributions of transition barriers for H interstitial diffusion between neighbouring sites. The large variation in the distributions is a result of the presence of Ga in the system. Mean values are (a) 0.42 eV, (b) 0.32 eV, (c) 0.33 eV and (d) 0.22 eV.

dral to octahedral is a likely diffusion pathway. Comparing the values we calculated for H interstitial diffusion to previously calculated values for Pu point defects (for example, 1.29 eV for a Pu vacancy and 0.96 eV for a (100) split interstitial [16]) shows that the H diffusion barriers are much smaller and will therefore occur over much smaller time scales.

3.2. Diffusivity in undamaged Pu-Ga

Before considering the effect of point defects on the diffusivity of H we initially calculated its diffusivity in a reference, undamaged material. The initial calculations were carried out in Pu 5 at. % Ga, before extending this to cover a range of Ga concentrations from 1 to 10 at. %. To obtain the diffusivity we first calculated the mean square displacement (MSD) for a range of temperatures, as discussed in the methodology section. The diffusivity was
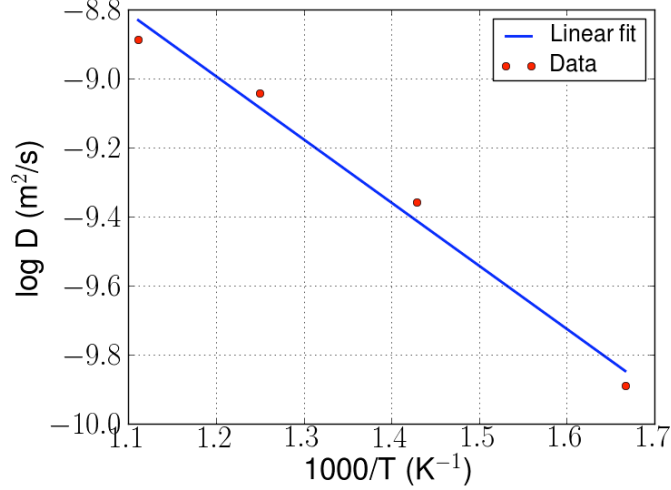
Figure 2: Arrhenius plot of the diffusivity of H in Pu 5 at. % Ga against temperature. Diffusivity increases with temperature with good linear correlation.

then obtained from the time dependence of the MSD (see Equation 3) and is shown in Figure 2, where the straight line confirms Arrhenius behaviour. We next calculated the effective migration energy barrier from the temperature dependence of the diffusivity (see Equation 4). The effective migration energy barrier for this case was found to be 0.36 eV. The Arrhenius plot and migration energy barrier were similar to other work that has been carried out on H diffusion in FCC metals [32], where the authors find the migration energy barriers of H in Al and Ni to be 0.39 and 0.56 eV respectively.

Figure 3 highlights the effect of Ga concentration on H diffusion. Although the average Ga concentration within the system was 5 at. %, due to the random Ga arrangement within the system there exist localised regions of higher (and lower) Ga concentration. In the figure we have indicated such high concentration regions by the dark blue volumes. Other coloured spheres represent the positions of the H atoms at all time points of the simulation (i.e. every site they visited during the simulation). From the figure it is clear that the H atoms would not enter into a region of high Ga concentration and, furthermore, that the diffusion pathways were affected by these high Ga concentration regions. For example, the purple H atom diffused towards a high Ga concentration region whereupon its direction of diffusion was reversed. This is an interesting finding since the Ga distribution in Pu-Ga is known to

10

Ga concentration (at. %)	Migration energy barrier (eV)
1	0.29
3	0.34
5	0.36
10	0.43

Table 2: Effective migration energy barriers for H in different concentrations of Ga, showing the barriers increase with Ga concentration. This is because there are fewer diffusion pathways available at these higher concentrations as the H atoms will not diffuse through localised regions of high Ga concentration.

be non-uniform. Grain boundaries are known to be Ga-poor while the grain centres have higher concentrations of Ga [28, 33]. This could lead to grain boundaries becoming a channel for H diffusion in the system. Previous work on point defect diffusion in Pu-Ga observed a similar effect; vacancies and Pu interstitials will not diffuse into a region of high Ga concentration [16] but are instead confined to regions of high Pu concentration.

Since we have shown that the local Ga concentration within the alloy had an effect on H diffusion, we next investigated changes to the system Ga concentration on H diffusion. We varied the Ga concentration from 1 to 10 at. % to obtain a range of values. Arrhenius plots for the different Ga concentrations are shown in Figure 4 with the corresponding migration energy barriers shown in Table 2. This clearly shows that as Ga concentration increased H diffusivity decreased. This is caused by a reduction in the number of diffusion pathways (between high Ga concentration regions) available to the H atoms. This could be an important finding with one implication being that you might expect to see high H diffusion at grain boundaries, which are Ga-poor, and lower H diffusion at the grain core. Also, if you were able to control Ga concentration within the system then you could potentially control H diffusion. In short, wherever Ga concentration varies in the material this has implications for H diffusion.

3.3. Interaction of H with point defects

With a view to understanding the effect of damage on H diffusion we have investigated the interaction between a H interstitial atom and both a vacancy and a Pu split interstitial. We have used both MD diffusivity simulations and binding energy calculations to investigate these interactions.
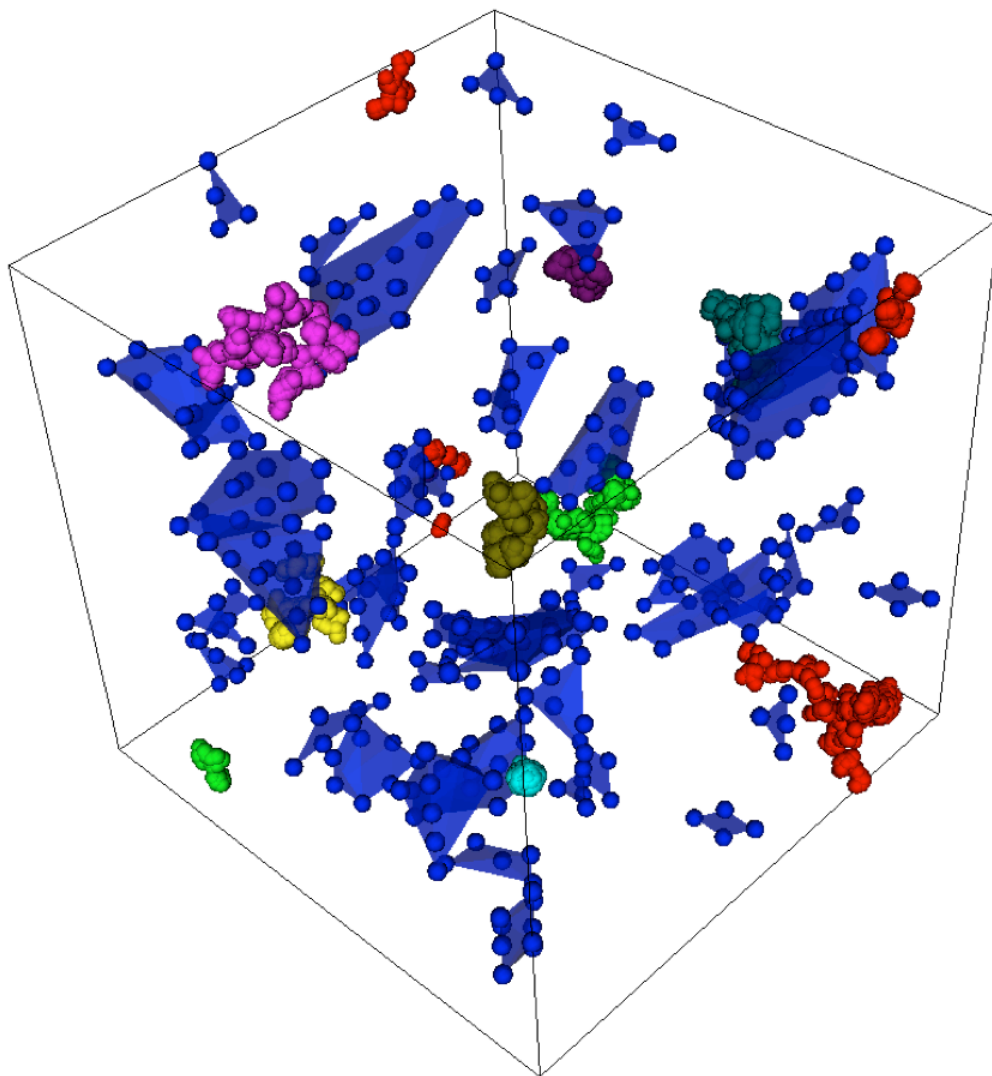
Figure 3: H avoiding regions of high Ga concentration. Dark blue volumes (and atoms) indicate regions of high Ga concentration. Spheres of the same colour indicate the position of an individual H atom at all time points of the simulation (there were 8 H atoms in each simulation). The red and purple H atoms are good examples of regions of high Ga concentration effecting H diffusion pathways.
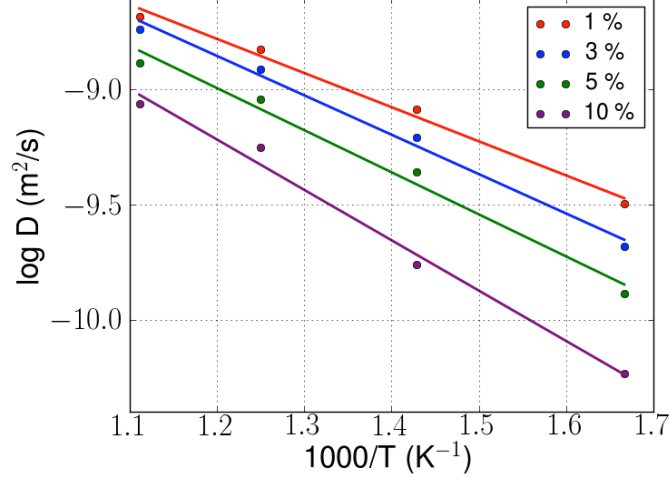
Figure 4: Arrhenius plot of the diffusivity of H for different Ga concentrations (1, 3, 5 and 10 at. %). As temperature increases so does diffusivity, whereas diffusivity decreases for increasing Ga concentration.

We have first considered the interaction of a H interstitial with a Pu vacancy and have initially performed MD diffusivity simulations on systems containing a H interstitial and a Pu vacancy. Figure 5 shows the distributions of the separations between the vacancy and the H interstitial, from the beginning and end of the simulations. From Figure 5(a) it appears as though there was an unstable region within approximately 3 Å of the vacancy. H atoms within the first two bars (2 Å) were classed as being within the vacancy and no atoms were initially within the 2-3 Å bin. Systems were created with separations in this range but during the minimisation phase (after initially creating the defects) the H atoms relaxed straight into the vacancies, indicating this region was unstable. The distribution of final separations (Figure 5(b)) also indicates this to be the case. After a time of 300 ps very few H atoms remained within 5 Å of the vacancy that were not captured and the number of captured H atoms grew substantially. The distribution was more spread out after 300 ps which suggests there was no long range interaction between the two defects. During the simulations we did not observe the dissociation of a H atom once it was captured by the vacancy. Nearly all H atoms that were initially within 6 Å of a vacancy were captured by the vacancy within 300 ps.
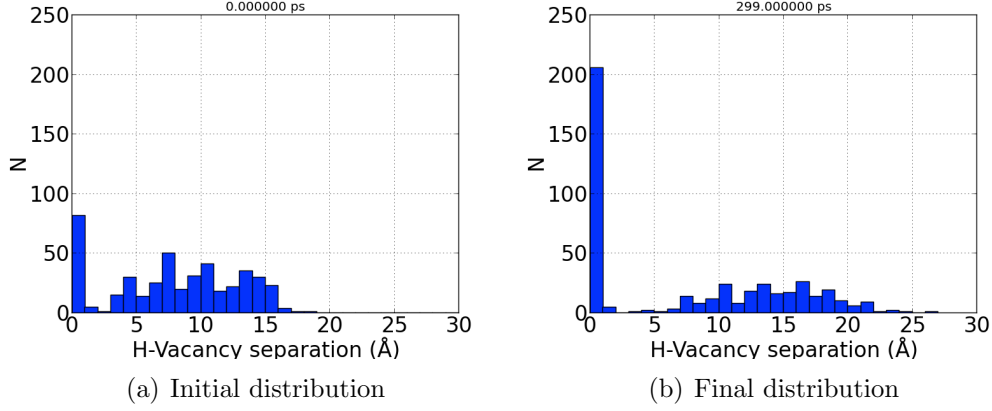
(a) Initial distribution
(b) Final distribution

Figure 5: Distributions of separations between the H interstitial and Pu vacancy during the diffusion simulations. The large increase in the first bar is a result of H atoms being captured by the vacancies.

To further investigate the capture radius of a Pu vacancy we calculated the binding energy of a H atom to the vacancy. To do this we needed to know the energy of the defects when they were well separated, which we took to be the sum of the Pu vacancy DFE (0.62 eV [16]) and the mean H interstitial energy with the perfect lattice as a reference (1.88 eV, from Table 1). The results of this calculation are shown in Figure 6 and clearly indicate that the H sitting in the vacancy was very energetically favourable; on average this was approximately 1.8 eV lower in energy than when the defects were well separated. There were no stable sites within 3 Å of the vacancy. Thus if a H atom were to enter this region it would be captured by the vacancy and would be very unlikely to dissociate. However there did not appear to be a longer range binding between the vacancy and the H, since outside the 3 Å capture radius the binding energy was constant at approximately 0 eV. It might be expected that the strain field of the vacancy would effect the H at a greater distance, however, perhaps the small size of the H relative to Pu-Ga negated this effect. This finding has important implications when considering the diffusivity of H in cascade damaged Pu-Ga. When a H atom is diffusing through an undamaged region of the system its diffusion coefficient will be as we calculated for the undamaged material (Section 3.2), depending on the local Ga concentration; if the H atom were to encounter a vacancy it would become trapped by the vacancy and its diffusion coefficient would effectively
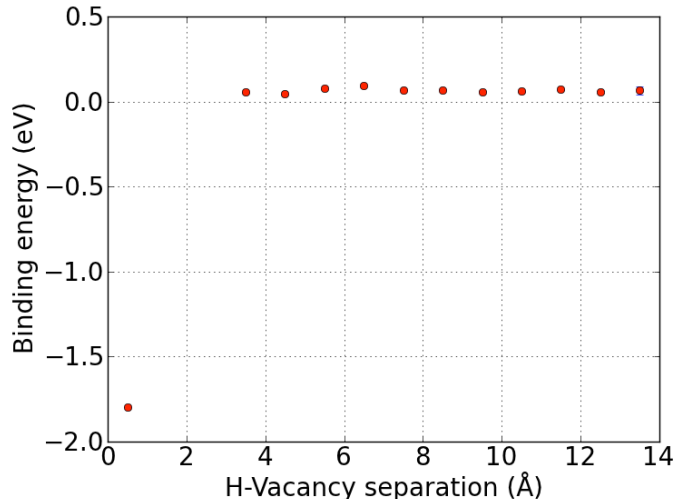
14

Figure 6: H - Pu vacancy binding energy results showing the mean binding energy in bins of 1 Å (75, 000 calculations in total). The standard error is within the points.

become zero. Transition barrier searches (see [34]) on the H-vacancy complex found the lowest energy barrier for a H to dissociate was approximately 1.8 eV, which is very unlikely to occur on relevant time scales and temperatures. For example, at 350 K this transition will occur approximately once every 260, 000 years, although at higher temperature it will occur more frequently – once per millisecond at 900 K.

The interaction of a H atom with a Pu interstitial was investigated in the same manner as the H - Pu vacancy simulations, with the vacancy replaced by a Pu split interstitial. Figure 7 shows the H - Pu interstitial separations at the beginning and end of the MD diffusivity simulations. The initial distribution indicates no H atoms were formed within 2 Å of the Pu interstitial but a large number were formed between 3-4 Å. This was due to atoms created within 2 Å moving away from the interstitial during the initial minimisation phase of the defective system and indicates sites within this range were unstable. At the end of the simulation there were still no H atoms within 2 Å of the interstitial and the distribution of separations has levelled out, suggesting there was no long range interaction.

As in the H - Pu vacancy case we have also calculated the binding energy of the H to the Pu interstitial. The mean binding energy as a function of sep-

15

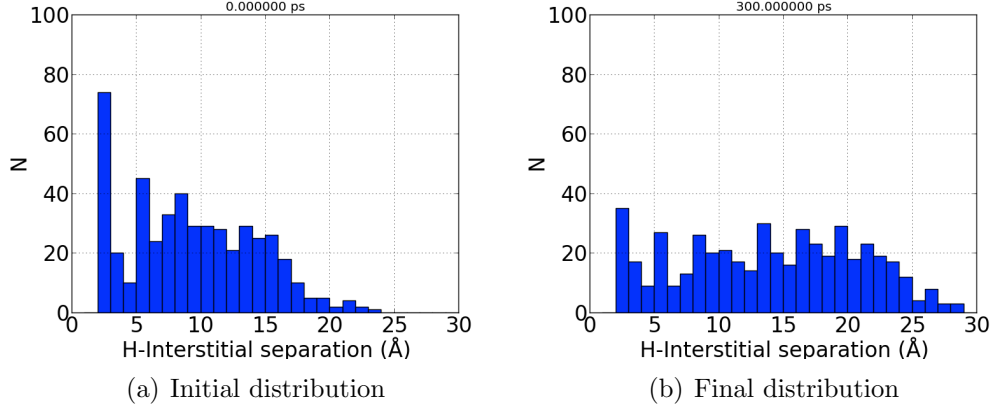(a) Initial distribution (b) Final distribution

Figure 7: Distributions of separations between the H interstitial and Pu interstitial during the diffusion simulations.

aration is shown in Figure 8. When the separation was within 2 Å the energy of the system was approximately 0.4-0.5 eV higher than at greater separations, which explains why no separations within this range were observed during the simulations. Therefore, whereas there was a binding between a H and a vacancy, there was no binding between an interstitial and a H. In fact the two did not like to be near each other. One possible implication of this is that a H-vacancy complex may block the recombination of Pu interstitials with vacancies that neighbour the complex. Once more there did not appear to be any longer range effects between the Pu defect and H atom.

4. Conclusions

An investigation into the diffusivity of H in Ga stabilised δ-Pu has been carried out. Calculations of H-Pu/Ga energetics have shown that the average energy of a H interstitial is less than that of a H sitting substitutionally with a neighbouring Pu interstitial. Allied with the low energy barriers of H interstitial transitions this suggests that H will diffuse freely between interstitial sites in an undamaged Pu-Ga system.

However, MD diffusivity simulations have shown this not to be the case. While H diffusivity does increase with temperature as expected, it has been shown that local Ga concentration has a substantial effect on H diffusivity. Regions of high Ga concentration were identified within the systems and we observed that H atoms would never enter these regions. Instead they must
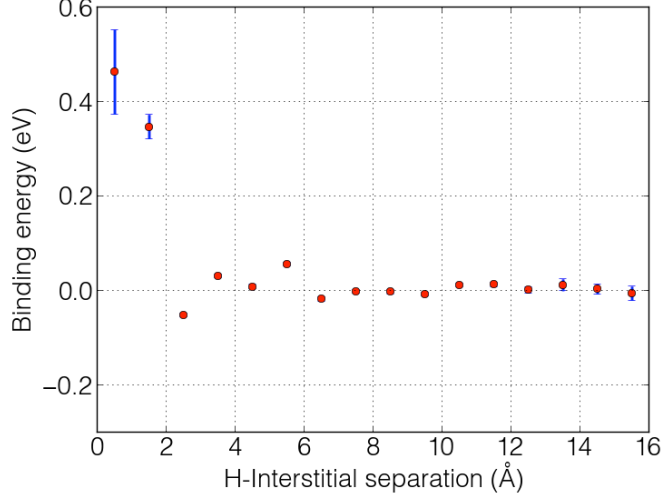
16

Figure 8: H - Pu interstitial binding energy results showing the mean binding energy in bins of 1 Å. Where the error bars are larger this is a result of less data being available for these points.

find diffusion pathways between them. The effect of increasing the system wide Ga concentration on H diffusion was then investigated. It was shown that as Ga concentration increased the H diffusion coefficient decreased. This was due to there being more regions of high Ga concentration and therefore fewer pathways between them. This finding could have significant implications on H diffusivity at grain boundaries, which are known to be Ga-poor.

Finally we have investigated the interaction of H with simple point defects. Diffusivity simulations containing a H interstitial and Pu vacancy, and binding energy calculations with the two defects, have shown that a vacancy will trap the H atom if it comes within approximately 3 Å of it. Outside this separation there did not appear to be any long range interaction between the defects, possibly due to the small size of the H atom in comparison to Pu-Ga. The opposite effect was observed for a Pu interstitial and H. In this case it was energetically unfavourable for the H to be within 2 Å of the Pu interstitial. These findings suggest that H diffusivity in cascade damaged material will be different to the undamaged case, since once a H enters the vicinity of a vacancy it will be captured and is very unlikely to dissociate, effectively reducing its diffusion coefficient to zero, assuming the combined hydrogen-vacancy complex does not diffuse. It could also result in an increase

17

in residual damage since Pu interstitials may not be able to recombine with vacancies that are near, or combined with, a H atom, due to the repulsion between the H and Pu interstitials.

In this work we have begun to investigate the behaviour of H in aged Pu. Thus far we have only considered the interaction of H with single Pu point defects and we wish to extend this to eventually investigate the interaction of H with cascade damaged Pu-Ga systems. The next step will be to look at the interaction of H, or multiple H, with multiple vacancies. We also intend to introduce He to the system in order to investigate site competition between H and He. The development of long time scale dynamics techniques [34] will also allow us to model H diffusivity in the cascade damaged material over realistic time scales.

Acknowledgements

References

[1] L. R. Morss, N. M. Edelstein, J. Fuger, The Chemistry of the Actinide and Transactinide Elements, volume 2, 3rd ed., Springer, 2006.

[2] S. Hecker, D. Harbur, T. Zocco, Prog. Mater. Sci. 49 (2004) 429–485.

[3] R. A. Oriani, Ann. Rev. Mater. Sci. 8 (1978) 327–57.

[4] P. Scott, J. Nucl. Mat. 211 (1994) 101–122.

[5] G. Young, J. Scully, Acta Mater. 46 (1998) 6337–6349.

[6] B. Hohler, H. Schreyer, J. Phys. F: Met. Phys. 857 (2000) 857–874.

[7] W. Wade, J. Nucl. Mat. 38 (1971) 292–302.

[8] M. Robinson, Simulating Radiation Damage in Plutonium, Ph.D. thesis, Loughborough University, 2010.

[9] M. I. Baskes, Phys. Rev. B 62 (2000) 1–6.

[10] V. Dremov, F. Sapozhnikov, S. Samarin, D. Modestov, N. Chizhkova, J. Alloys Compd. 444-445 (2007) 197–201.

[11] M. Baskes, J. Nelson, A. Wright, Phys. Rev. B 40 (1989) 6085.

[12] M. I. Baskes, K. Muralidharan, M. Stan, S. M. Valone, F. J. Cherne, JOM 55 (2003) 41–50.

[13] S. M. Valone, M. I. Baskes, R. Martin, Phys. Rev. B 73 (2006) 1–11.

[14] M. Robinson, S. D. Kenny, R. Smith, M. T. Storr, Nucl. Instrum. Methods Phys. Res., Sect. B 269 (2011) 2539–2548.

[15] M. Robinson, S. D. Kenny, R. Smith, M. T. Storr, E. McGee, Nucl. Instrum. Methods Phys. Res., Sect. B 267 (2009) 2967–2970.

[16] M. Robinson, S. D. Kenny, R. Smith, M. T. Storr, J. Nucl. Mat. 423 (2012) 16–21.

[17] B. P. Uberuaga, S. M. Valone, M. Baskes, J. Alloys Compd. 444-445 (2007) 314–319.

[18] L. Berlu, G. Jomard, G. Rosa, P. Faure, J. Nucl. Mat. 372 (2008) 171–176.

[19] D. S. Schwartz, S. Richmond, A. I. Smith, A. Costello, C. D. Taylor, Mater. Res. Soc. Symp. Proc. 1444 (2012) 183–188.

[20] C. D. Taylor, S. C. Hernandez, M. F. Francis, D. S. Schwartz, A. K. Ray, J. Phys.: Condens. Matter 25 (2013) 265001.

[21] H. Y. Wei, S. Z. Luo, G. P. Liu, X. L. Xiong, H. T. Song, Acta Phys. -Chim. Sin. 24 (2008) 1964–1968.

[22] L. Berlu, G. Jomard, G. Rosa, P. Faure, J. Nucl. Mat. 374 (2008) 344–353.

[23] S. M. Valone, M. I. Baskes, M. Stan, T. E. Mitchell, A. C. Lawson, K. E. Sickafus, J. Nucl. Mat. 324 (2004) 41–51.

[24] M. I. Baskes, Phys. Rev. B 46 (1992) 2727–2742.

[25] J. F. Ziegler, J. P. Biersack, U. Littmark, The Stopping and Range of Ions in Matter, Pergamon, New York, 1985.

[26] S. M. Valone, M. I. Baskes, J. Comput. Aided Mater. Des. 14 (2007) 357–365.

[27] M. I. Baskes, S. Y. Hu, S. M. Valone, G. F. Wang, A. C. Lawson, J. Comput. Aided Mater. Des. 14 (2007) 379–388.

[28] S. S. Hecker, Los Alamos Science 26 (2000) 290–335.

[29] C. Zhu, R. H. Byrd, J. Nocedal, ACM T. Math. Software 23 (1997) 550–560.

[30] G. Henkelman, B. P. Uberuaga, H. Jónsson, J. Chem. Phys. 113 (2000) 9901.

[31] H. J. C. Berendsen, J. P. M. Postma, W. F. van Gunsteren, J. R. Haak, J. Chem. Phys. 81 (1984) 3684.

[32] W.-S. Ko, J.-H. Shim, B.-J. Lee, J. Mater. Res. 26 (2011) 1552–1560.

[33] J. L. Robbins, J. Nucl. Mat. 324 (2004) 125–133.

[34] C. Scott, S. Blackwell, L. Vernon, S. D. Kenny, M. Walls, R. Smith, J. Chem. Phys. 135 (2011) 174706.